Weathering Performance of Wood Coated with a Combination of Alkoxysilanes and Rutile TiO_2 Heirarchical Nanostructures

Rongbo Zheng,[a,b,*] Mandla A. Tshabalala,[c,*] Qingyu Li,[a] and Hongyan Wang[d]

The weathering performance of wood coated with a combination of rutile TiO_2 hierarchical nanostructures and a sol-gel deposit of alkoxysilanes was determined by exposing three sets of specimens to UV light and water spray. The first set consisted of specimens coated with a mixture of methyltrimethoxysilane (MTMOS) and hexadecyltrimethoxysilane (HDTMOS). The second set consisted of specimens coated with nanostructural TiO_2 followed by a mixture of MTMOS and HDTMOS. The third set consisted of uncoated control specimens. The wood coated with TiO_2 followed by a mixture of MTDMOS and HDTMOS exhibited significantly less surface color change and weight loss as a result of UV light-induced degradation and erosion from water spray in comparison with the other groups. However, the coated surfaces were gradually transformed from hydrophobic to hydrophilic. Despite this apparent weakness, the MTMOS/HDTMOS/TiO_2 coating, with superior photostabilization properties and resistance to surface erosion, may be useful for improving the weathering performance of wood coated with semi-transparent wood stains.

Keywords: *Coating; Hydrophobic; Nanostructure; Photostabilization; Rutile; Titanium dioxide; Weathering; Wood*

Contact information: *a: College of Science, Southwest Forestry University, Kunming 650224, P. R. China; b: Wood Adhesives and Glued Products Key Laboratory of Yunnan Province, Southwest Forestry University, Kunming 650224, P. R. China; c: U.S. Department of Agriculture, Forest Service, Forest Products Laboratory, One Gifford Pinchot Drive, Madison, WI 53726-2398, USA; d: Zhejiang Forestry Academy, Hangzhou 310023, P.R. China;*
** Corresponding authors: zhengrbzy@hotmail.com; mtshabalala@fs.fed.us*

INTRODUCTION

When wood materials are used outdoors without protection, they undergo degradation from the effects of sunlight and water. The deterioration of the wood surface caused by exposure to sunlight and rain is referred to as weathering. The major elements in wood weathering are UV radiation, water, heat, and erosion (Feist and Hon 1984). The UV radiation causes photochemical degradation primarily in the lignin component of the wood cell wall and gives rise to characteristic color changes that depend on the wood species. Lodgepole pine, for example, changes from a light yellow natural color to brown and, eventually to gray. Also as the lignin is degraded, the wood surface becomes richer in cellulose content. Water plays a major role in the weathering of wood. As the lignin is broken down, water leaches out lignin degradation products. Water also washes away surface cellulose fibers that have been released due to the lignin degradation resulting in wood surface erosion.

Approaches to improving the weathering performance of wood and preserving its aesthetic qualities are being continually refined, and new such approaches are being developed. These include nanosol treatment (Mahltig *et al.* 2008; Xu *et al.* 2010;

Tshabalala *et al.* 2011), the plasma-enhanced chemical vapor deposition of thin barrier films onto the wood surface (Denes *et al.* 1999), and hydro/solvothermal treatment (Li *et al.* 2010). Recently, there has been a renewed interest in the use of titanium dioxide nanostructures in combination with surface-active organic compounds to enhance the UV resistance and water repellence properties of wood surfaces (Wang *et al.* 2011; Chu *et al.* 2014; Wang *et al.* 2014).

Titanium dioxide exists in three crystalline forms: anatase, rutile, and brookite, which differ from one another in photocatalytic activity (Addamo *et al.* 2006). The photocatalytic activity is greatest in brookite, followed by anatase, then rutile. Allen *et al.* (2004) reported that titanium dioxide nanoparticles in the form of rutile, when incorporated into clear acrylic wood coating, are more effective than their other crystalline forms in protecting wood against degradation by UV light. This may be explained by the theory that rutile operates primarily as a photostabilizer, whereas brookite and anatase operate primarily as photosensitizers. The anatase form has been used as a photocatalyst for lignin degradation in solution (Tanaka *et al.* 1999). Another study showed that the partial delignification of wood surfaces by treatment with peracetic acid resulted in enhanced photostability because of the decomposition of surface UV-absorbing lignin (Dawson *et al.* 2000). The objective of the present study was to test the hypothesis that a similar effect, facilitated by using rutile TiO_2 nanostructures as a coating, can be achieved by the photolytic delignification of the cell walls in the surface layers of the wood substrate. Thus, the wood surface would be protected from discoloration by a dual mechanism: oxidative delignification and the restriction of access of the UV light to the wood surface via UV light absorption and scattering.

EXPERIMENTAL

Materials

Wood specimens were obtained from logs of mountain pine beetle-killed lodgepole pine (*Pinus contorta* Dougl.). The specimens were cut into wafers measuring 1.0 mm × 15.8 mm × 51.3 mm in the tangential, radial, and longitudinal directions, respectively. The 12% $TiCl_3$ solution, hexadecyltrimethoxysilane (HDTMOS), and methyltrimethoxysilane (MTMOS) were obtained from Sigma-Aldrich. All other laboratory chemicals used were obtained from various suppliers and were (ACS) reagent grade.

Methods

Coating with rutile Ti02 nanostructures

Wood specimens that had been previously equilibrated at 30% relative humidity were coated with rutile Ti02 nanostructures by means of a room temperature oxidative reaction with $TiCl_3$ in saturated NaCl aqueous solution (Zheng *et al.* 2015). Typically, 4 mL of $TiCl_3$ solution, which contained 12 wt.% $TiCl_3$ in hydrochloric acid, was dissolved in 120 mL of NaCl-saturated aqueous solution. The pH of the solution was adjusted by the addition of a solution of NaOH in saturated NaCl solution. After mixing for 12 h with a magnetic stirrer, six replicates of the wood wafers were placed in the coating solution and allowed to react for 10 days without stirring. After reaction, the specimens were rinsed with deionized water and allowed to dry under ambient conditions.

Coating with MTMOS and HDTMOS

Ethanol was mixed with a solution of MTMOS and a solution of HDTMOS in the volume ratio of 100:1:1 (95% ethanol: MTMOS: HDTMOS). Wood specimens were placed in the coating solution to react overnight at room temperature. After the reaction, the specimens were rinsed with ethanol and dried for 6 h in an oven at 65 °C before conditioning at 105 °C for 24 h.

Accelerated weathering

For accelerated weathering studies, six replicates each of the control uncoated (BW), HDTMOS/MTMOS-coated (HMW), and HDTMOS/MTMOS/TiO_2-coated (HMTW) wood specimens were exposed in the Ci-65 Weather-Ometer™ for a total of 960 h to Program 1, which consisted of a 2-h cycle (102 min of UV radiation followed by 18 min of radiation combined with water spray at 0.2 L min^{-1}). The light source was a xenon arc lamp with borosilicate inner and outer filters, and its irradiance at 340 nm was set at 0.35 W/m^2. The light-only black panel temperature (BPT) was 65 ± 2 °C, and the relative humidity (RH) was 48 ± 5 %. The light and spray BPT was 50 ± 5 °C, and the RH was 80 ± 5 %.

To determine the weight loss resulting from surface erosion, specimens were removed from the Weather-Ometer™ at predetermined intervals, preconditioned first at 30% RH and then weighed to equilibrium weight at 65% RH. The weight percent change was calculated according to Eq. 1,

$$\text{Weight percent change} = 100\,(W_1 - W_0)/\,W_0 \quad (1)$$

where W_0 and W_1 are the equilibrium weights before and after exposure in the Weather-Ometer™, respectively.

Surface characterization

The surface water repellence properties of the wood specimens before and after accelerated weathering were characterized by the dynamic contact angle measurement of a 4-μL deionized water droplet using a PGX+ Contact Angle Tester (Thwing-Albert Instrument Company, USA). The water contact angle (WCA) for each specimen was determined by taking the average of three measurements made at three different locations on each specimen. There were six replicates per treatment.

The surface morphology of the specimens was obtained by scanning electron microscopy (SEM) on a LEO 1530 field emission scanning electron microscope (Carl Zeiss AG). The crystalline phase of Ti02 was determined by X-ray Diffraction (XRD) (DX-2700, Rigaku) with Cu $K\alpha$ radiation (λ = 1.5418 Å). The surface chemistry was characterized by attenuated total reflectance Fourier transform infrared spectroscopy (ATR-FTIR) and energy dispersive X-ray analysis (EDXA). ATR-FTIR spectra were obtained on a Nicolet iZ module (Thermo Scientific) using a Smart iTR Basic accessory. The EDXA was performed on a LEO EVO40 scanning electron microscope with an attached Vantage EDX Analyzer (Carl Zeiss AG).

Surface color measurements were made in the CIE *L*a*b** color space with a Minolta CR-400 Chroma Meter (Osaka, Japan). The *L**, *a**, and *b** parameters for each specimen were measured at three contiguous locations on the surface of each specimen before and after exposure in the Weather-Ometer™. Changes in the *L**, *a**, and *b** parameters were calculated according to Eqs. 2 through 4,

$$\Delta L^* = L^*_{(w)} - L^*_{(u)} \quad (2)$$

$$\Delta a^* = a^*_{(w)} - a^*_{(u)} \quad (3)$$

$$\Delta b^* = b^*_{(w)} - b^*_{(u)} \quad (4)$$

where ΔL^*, Δa^*, and Δb^* are the differences between the weathered (w) and unweathered (u) surfaces. A positive value signifies an increase, whereas a negative value signifies a decrease. The corresponding total color difference was calculated according to Eq. 5.

$$\Delta E^* = \{\Delta L^{*2} + \Delta a^{*2} + \Delta b^{*2}\}^{1/2} \quad (5)$$

Higher values of ΔE^* signify greater discoloration.

RESULTS AND DISCUSSION

Rate of Weight Loss Following Exposure to Artificial Weathering

In a previous study, Tshabalala *et al.* (2003) found that a sol-gel deposit of a mixture of MTMOS and HDTMOS decreased the weight loss of wood exposed to weathering. The results of the present study suggested that specimens coated with a combination of Ti02 nanostructures and a mixture of MTMOS and HDTMOS (HMTW) may perform slightly better in terms of preventing weight loss caused by weathering-induced surface erosion. The rate of weight loss (Fig. 1) was highest for BW, followed by HMW, then HMTW. Thus, the presence of rutile Ti02 nanostructures covered with a thin film of a mixture of MTMOS and HDTMOS resulted in substantial improvement in resistance of the wood surface to weathering.

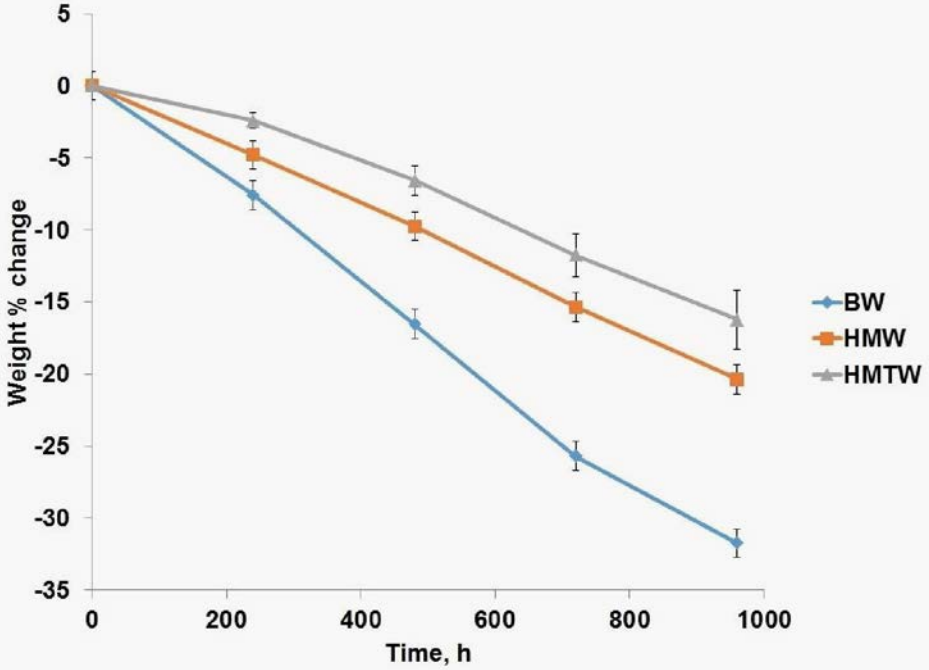

Fig. 1. Rates of weight loss of uncoated (BW), HDTMOS/MTMOS-coated (HMW), and HDTMOS/MTMOS/TiO_2-coated (HMTW) wood specimens

The ability of rutile Ti02 nanostructures to improve the wood surface resistance to weathering may have been related to a combination of three factors: the morphology of the Ti02 coating on the wood surface, the UV-screening properties of rutile TiO_2, and the photocatalytic properties ofrutile TiO_2, which could facilitate the photolytic delignification of the cell walls in the surface layers of the wood substrate.

SEM micrographs show the wood surface before (Fig. 2A) and after (Fig. 2B) coating with rutile TiO_2. The coated surface showed 1-µm rutile microspheres decorated with 20-nm to 100-nm nanospheres that are similar to the water repellent protrusions on the surface of a lotus leaf (Patankar 2004; Zhao *et al.* 2006)

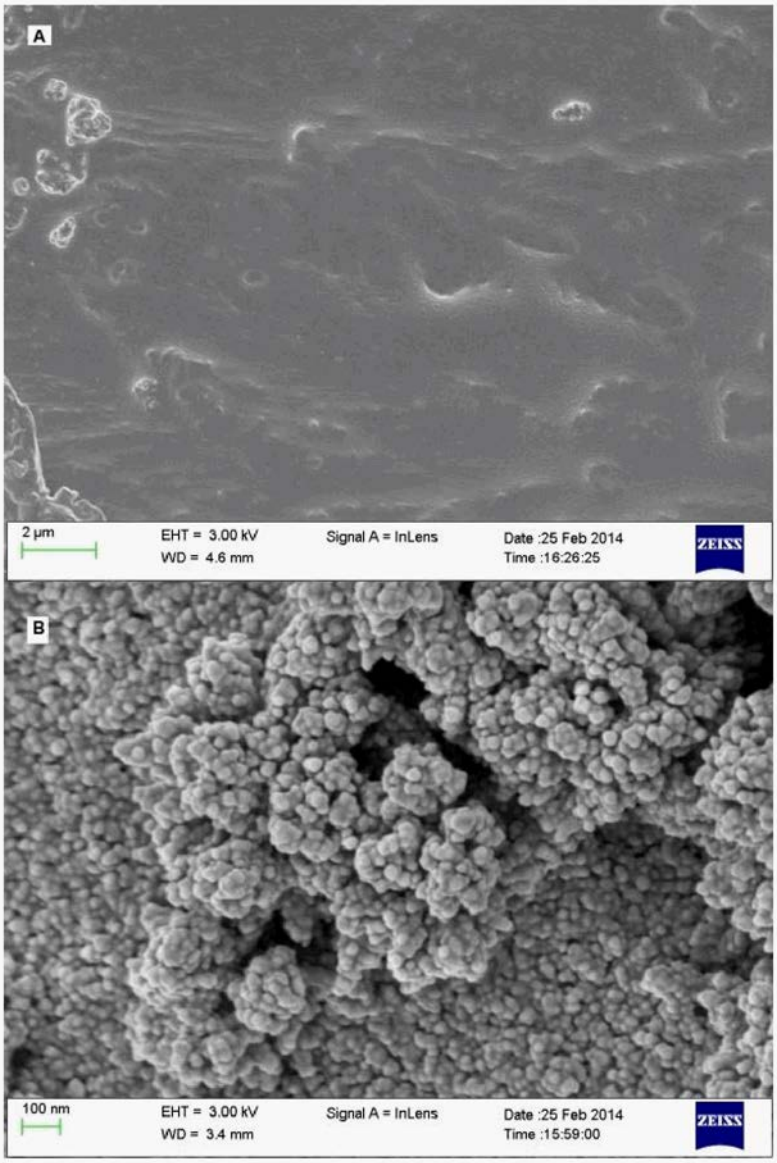

Fig. 2. SEM micrographs of (A) uncoated and (B) rutile TiO_2-coated wood specimens

The X-ray diffraction pattern (Fig. 3A) of the coated wood confirmed the crystallinity of the coating to be rutile (Fig. 3B). The peak labeled W (Fig. 3A) can be indexed to the diffraction pattern of wood.

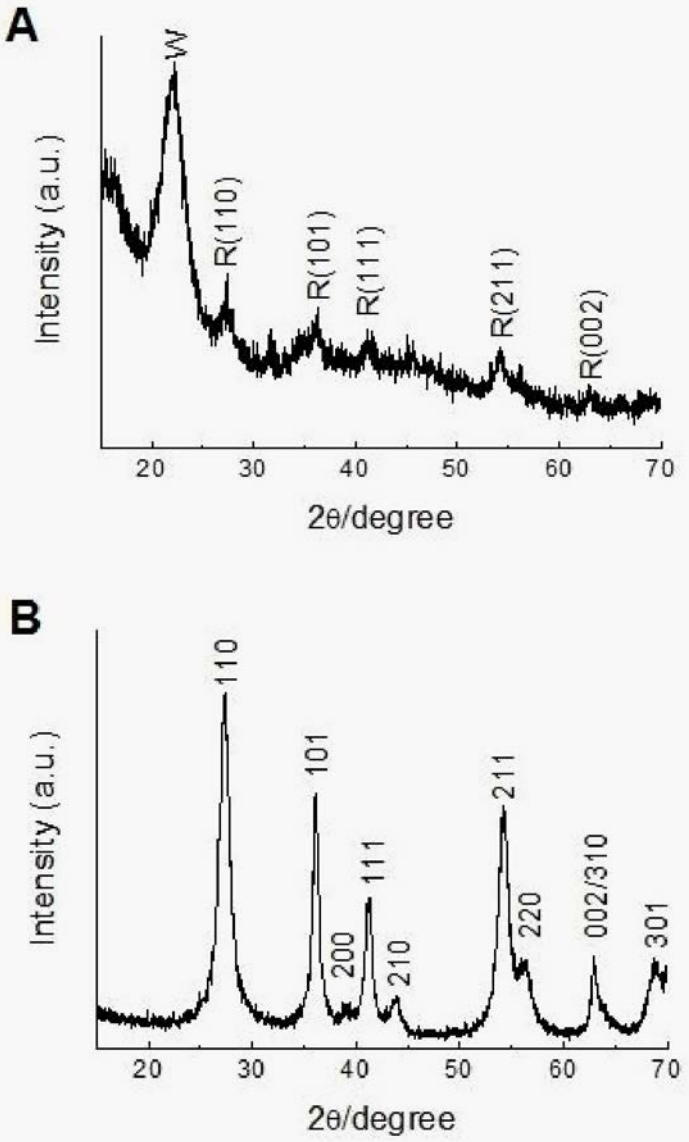

Fig. 3. X-ray diffraction patterns of (A) rutile TiO_2 coating on wood and (B) crystalline rutile TiO_2

Color Change

During the initial 240-h exposure, the rate of total color change, ΔE^*, of the specimens coated with rutile nanostructures (HMTW) was slightly higher than that of the uncoated controls (BW) or that of the specimens coated with only HDTMOS/MTMOS (HMW). Thereafter, the color change of the HMTW progressed at a much slower rate than did that of the BW or HMW (Fig. 4A). These differences in total color change between the uncoated (BW) and coated specimens (HMW or HMTW) were the result of complex and varying changes in the color parameters, ΔL^* (Fig. 4B), Δa^* (Fig. 4C), and Δb^* (Fig. 4D), induced by the accelerated weathering.

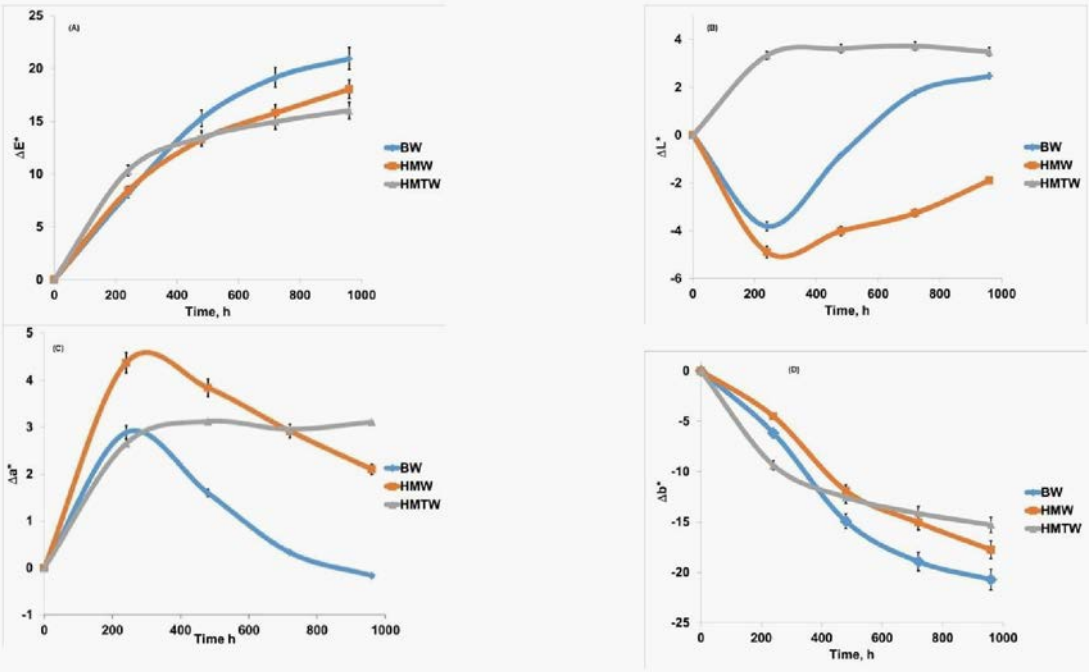

Fig. 4. (A) Total color change; (B) lightness change; (C) redness change; (D) yellowness change of specimens with exposure time in the Weather-Ometer™

For uncoated control specimens (BW), the total color change was most strongly influenced by the large decrease in Δb^* (shift to blue), and less strongly influenced by the slight increase in Δa^* (shift to redness) and the slight decrease in ΔL^* (lightness). During the course of the 960-h accelerated weathering, ΔL^* first decreased to a minimum of minus 3.82 ± 1.42, and then increased to a level of approximately 2.48 ± 1.80. In contrast, over the course of the 960-h accelerated weathering, Δa^* first increased to a maximum of 2.89 ± 0.28, and then decreased to a level of approximately zero after 960-h accelerated weathering.

For specimens coated with HDTMOS/ MTMOS alone (HMW), the total color change was influenced by the relatively smaller decrease in Δb^* compared with BW. However, ΔL^* decreased to a lower level of -4.90 ± 1.60 before increasing to approximately zero. Δa^* first increased to a higher level of 4.37 ± 0.62 before decreasing to a level of 2.10 ± 0.43 by the end of the 960-h accelerated weathering.

For specimens coated with rutile nanostructures (HMTW), the total color change was influenced by the small decrease in Δb^*, which was smaller than the decrease experienced by BW or HMW. Moreover, after the initial small increases, both ΔL^* and Δa^* remained practically constant for the rest of the 960-h exposure to UV irradiation and water spray.

Water repellent properties

It was expected that the enhanced water repellent properties of the coated wood surface would tend to limit access of the water spray to wash away the products of photodegradation induced by UV irradiation, and the UV-screening properties of rutile Ti02 would prevent UV radiation from reaching the wood surface, thus reducing the extent of surface photodegradation. Exposing the coated specimens, HMTW, to UV irradiation decreased the WCA from approximately 140° to about 15.9° (Table 1). This appeared to be consistent with observations made by Wang *et al*. (1999) and Feng *et al*. (2005) that photo-reduction of the surface Ti^{4+} to Ti^{3+} in the rutile TiO_2 nanostructures can result in the transformation of Ti02 film coating from a highly hydrophobic to either a hydrophilic or amphiphilic surface. When exposed to a combination of UV irradiation and water spray, both the uncoated and coated specimens suffered surface erosion that led not only to weight loss, but also changes in surface WCA, surface chemistry, and surface morphology.

Table 1. Water Contact Angles (WCA) of Uncoated and Coated Wood

Time / Specimen	0 h*	155 h**	960 h***
BW	28.2±3.7	24.5±2.0	≈0
HMW	116.7±14.6	102.8±7.0	43.3±8.6
HMTW	140.04±2.02	15.9±8.5	≈0
*Before exposure to UV light and water spray			
**After exposure to UV light only			
***After exposure to UV light and water spray			

Differences in surface chemistry of the uncoated (BW) and coated (HMW and HMTW) specimens are reflected in the IR spectra presented in Fig 5. The IR band assignments related to the different wood components are summarized in Table 2. The spectra of the coated specimens were quite different from that of the uncoated specimens. The most obvious differences were the weakening of all the bands for both HMW- and HMTW-coated specimens. Also in the case of HMTW-coated specimens, the band at 1724 cm^{-1} was absent, indicating hemicellulose degradation induced by treatment with TiO_2. The HMW-coated specimens on the other hand showed an additional band at 775 cm^{-1} (marked with an arrow), which was tentatively assigned to Si-O, Si-C or Si-O-C bonds (Bogart et al. 1998), indicating the presence of the alkoxysilane deposit.

After 960-h of exposure in the WeatherOmeter, the spectrum of the uncoated specimens (BW) was slightly different from the unweathered specimens. The most obvious difference was the increase in the intensity of the band at 1069 cm^{-1} indicating enrichment of the surface with cellulose as a result of the degradation and washing away of lignin. By comparison, for the specimens coated only with alkoxysilanes (HMW) the most obvious difference was the absence of the band at 775 cm^{-1}, indicating a partial washing away of the alkoxysilane. This apparently resulted in a slight enhancement of the bands at 1069 cm^{-1} and 3320 cm^{-1}. For the specimens coated with a combination of Ti02 and alkoxysilanes (HMTW), there was also a slight enhancement of bands at 1069 cm^{-1} and 3320 cm^{-1}, indicating surface exposure of the cellulose and an increase in bound water.

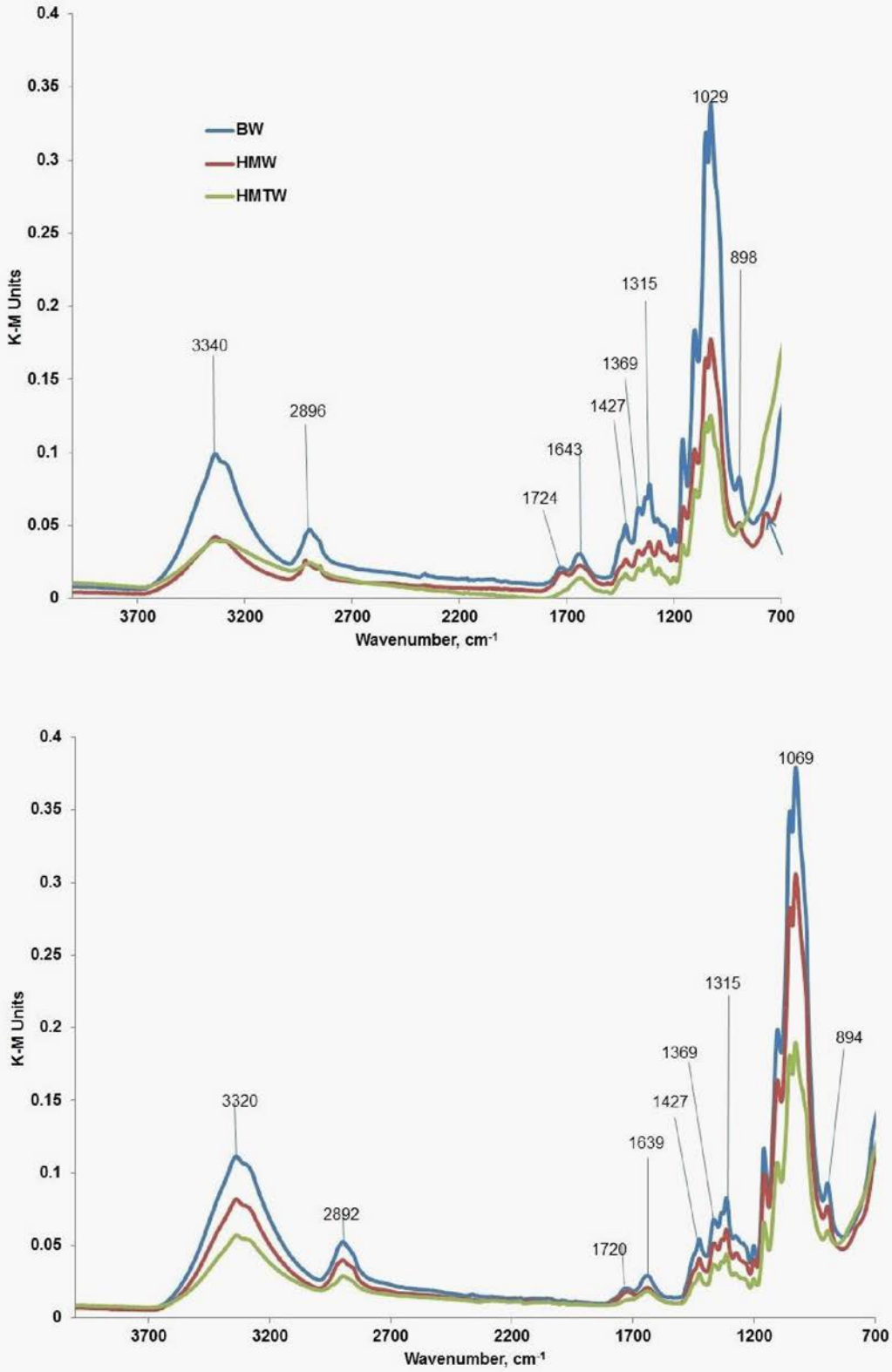

Fig. 5. ATR-FTIR spectra of uncoated (BW), HDTMOS/MTMOS-coated (HMW), and HDTMOS/MTMOS/TiO_2-coated (HMTW) wood specimens before and after 960-h exposure to UV irradiation and water spray

Table 2. Assignments of Bands in the Infrared Spectrum of Pine Wood

Wavenumber cm^{-1}	Assignment	Reference
3340	OH stretching in bound water	Tolvaj and Faix 1995
2896	CH and CH_2 stretching (asymm.)	Tolvaj and Faix 1995
1724	CO stretching in acetyl and carboxyl groups in hemicellulose	Evans *et al.* 1992
1643	H-O-H deformation in absorbed water in carbohydrates	Evans *et al.* 1992
1427	C-H deformation (asymm)	Tolvaj and Faix 1995
1369	CH bending in cellulose and hemicellulose	Evans *et al.* 1992
1315	CH_2 wagging in cellulose	Evans *et al.* 1992
1029	C_{alkyl} – O group in cellulose	Tolvaj and Faix 1995
898	C_1 – H deformation of cellulose	Tolvaj and Faix 1995

Surface erosion of specimens coated with rutile TiO_2 nanostructures was confirmed by EDXA. After 960-h exposure in the WeatherOmeter, the HMTW specimens showed a significant decrease in relative intensity of the titanium peak (Fig. 6).

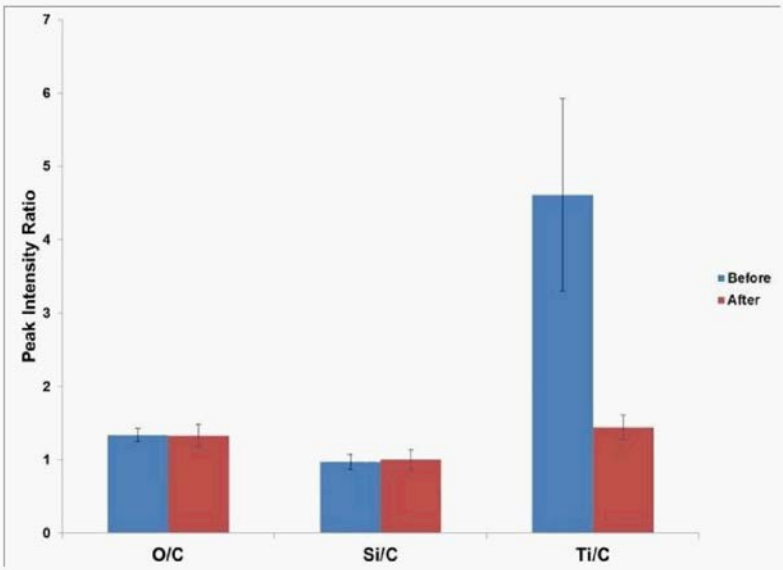

Fig. 6. EDX peak ratios of HDTMOS/MTMOS/TiO_2-coated wood before and after 960-h exposure to UV irradiation and water spray

CONCLUSIONS

1. Wood specimens coated with rutile TiO_2 and a mixture of methyltrimethoxysilane and hexadecyltrimethoxysilane showed superior weathering performance when compared with control uncoated specimens or specimens coated only with alkoxysilanes.

2. The specimens coated with rutile Ti02 and a mixture of methyltrimethoxysilane and hexadecyltrimethoxysilane showed improved resistance to surface color change and weight loss.
3. After 960-h exposure to UV radiation and water spray, the specimens showed a drastic decrease in surface water contact angle, and small losses of titanium from their surfaces.
4. Additional studies are required to improve the durability of these coatings to the effects of weathering

ACKNOWLEDGMENTS

The authors are grateful to Thomas Kuster and Philip Walsh at USDA Forest Products Laboratory for their support with microscopy and spectroscopy. Financial support from the National Natural Science Foundation of China (31100420, 30930074) and the Southwest Forestry University Foundation (110930) are gratefully acknowledged. This research was funded in part by the China Scholarship Council (CSC).

REFERENCES CITED

Addamo, M., Bellardita, M., Di Paola, A., Palmisano, L. (2006). "Preparation and photoactivity of nanostructured anatase, rutile and brookite Ti02 thin films," *Chem. Commun.* 4943-4945. DOI: 10.1039/B612172A

Allen, N. S., Edge, M., Ortega, A., Sandoval, G., Liauw, C. M., Verran, J., Stratton, J., McIntyre, R. B. (2004). "Degradation and stabilization of polymers and coatings: Nano versus pigmentary titania particles," *Polym. Degrad. Stab.* 85, 927-946. DOI: 10.1016/j.polymdegradstab.2003.09.024

Bogart, K. H. A., Ramirez, S. K., Gonzales, L. A., Bogart, G. R., and Fisher, E. R. (1998) "Deposition of Si02 films from novel alkoxysilane/O-2 plasmas," *J. Vac. Sci. Technol. A* 16(6), 3175-3184. DOI 10.1116/1.581517

Chu, T. V., Chuong, P. V., Tuong, V. M. (2014). "Wettability of wood pressure-treated with Ti02 gel under hydrothermal conditions," *BioResources* 9, 2396-2404. DOI: 10.15376/biores.9.2.2396-2404

Dawson, B. S. W., Singh, A. P., Kroese, H. W., Schwitzer, M. A., Gallagher, S., Riddiough, S. J., Wu, S. (2000). "Enhancing exterior performance of clear coatings through photostabilisation of wooden surfaces. Part 1: Treatment and characterization," *J. Coat. Technol. Res.* 5(2), 193-206. DOI: 10.1007/s11998-008-9089-5

Denes, A. R., Tshabalala, M. A., Rowell, R., Denes, F., Young, R. A. (1999). "Hexamethyldisiloxane-plasma coating of wood surfaces for creating water repellent characteristics," *Holzforschung* 53, 3 18-326. DOI: 10.1515/HF.1999.052

Evans, P. D., Michell, A. J., and Schmalzl, K. J. (1992). "Studies of the degradation and protection of wood surfaces," *Wood Sci. Technol.* 26, 151-163.

Feist, William C. and Hon, David N.-S. (1984) "Chemistry of weathering and protection," In: Rowell, Roger M., ed. The chemistry of solid wood. Advances in chemistry series 207. Washington, DC American Chemical Society; Chapter 1 1.

Feng, X. J., Zhai, J., Jiang, L. (2005). "The fabrication and switchable superhydrophobicity of TiO_2 nanorod films," *Angew. Chem. Int. Ed.* 44, 5115-5118. DOI: 10.1002/anie.200501337

Li, J., Yu, H. P., Sun, Q. F., Liu, Y. X., Cui, Y. Z., Lu, Y. (2010). "Growth of TiO_2 coating on wood surface using controlled hydrothermal method at low temperatures," *Appl. Surf Sci.* 256, 5046-5050. DOI: 10.1016/j.apusc.2010.03.053

Mahltig, B., Swaboda, C., Roessler, A., Böttcher, H. (2008). "Functionalising wood by nanosol application," *J. Mater. Chem.* 18, 3 180-3 192. DOI: 10.1039/b718903f

Patankar, N. A. (2004). "Mimicking the lotus effect: Influence of double roughness structures and slender pillars," *Langmuir* 20, 8209-821 3. DOI: 10.1021/1a048629t

Tanaka, K., Calanag, R. C. R., Hisanaga, T. (1999). "Photocatalyzed degradation of lignin on TiO_2," *J. Mol. Catal. A: Chem.* 138, 287-294. DOI: 10.1016/S1381-1169(98)00161-7

Tolvaj, L., Faix, 0. (1995). "Artificial ageing of wood monitored by DRIFT Spectroscopy and CIE *L* a* b** color measurements," *Holzforschung* 49, 397-404. DOI: 10.1515/hfsg.1995.49.5.397

Tshabalala, M. A., Gangstad, J. E. (2003). "Accelerated weathering of wood surfaces coated with multifunctional alkoxysilanes by sol-gel deposition," *J. Coat. Technol.* 75(943), 37-43. DOI: 10.1007/BF02730098

Tshabalala, M. A., Libert, R., Schaller, C. M. (201 1). "Photostability and moisture uptake properties of wood veneers coated with a combination of thin sol-gel films and light stabilizers," *Holzforschung* 65, 215-220. DOI: 10.1515/hf.2011.022

Wang, C. Y., Piao, C., Lucas, C. (2011). "Synthesis and characterization of superhydrophobic wood surfaces," *J. Appl. Polym. Sci.* 119, 1667-1672. DOI: 10.1002/app.32844

Wang, R., Sakai, N., Fujishima, A., Wanatabe, T., Hashimoto, K. (1999). "Studies of surface wettability conversion on TiO_2 single-crystal surfaces," *J. Phys. Chem. B* (103), 2188-2194. DOI: 10.1021/jp983386x

Wang, X. Q., Liu, S. C., Chang, H. J., Liu, J. L. (2014). "Sol-gel deposition of TiO_2 nanocoatings on wood surfaces with enhanced hydrophobicity and photostability," *Wood Fiber Sci.* 46, 109-117.

Xu, Q. F., Wang, J. N., Sanderson, K. D. (2010). "A general approach for superhydrophobic coating with strong adhesion strength," *J. Mater. Chem.* 20, 5961-5966. DOI: 10.1039/c0jm0001a

Zhao, N., Weng, L., Zhang, Q. X., Zhang, X., Xu, J. (2006). "A lotus leaf-like superhydrophobic surface prepared by solvent-induced crystallization," *ChemPhysChem.* 7, 824-827. DOI: 10.1002/cphc.200500698

Zheng, R. B., Meng, X. W., Tang, F. Q. (2009). "Synthesis, characterization and photodegradation study of mixed-phase titania hollow submicrospheres with rough surface," *Appl. Surf Sci.* 255, 5989-5994. DOI: 10.1016/j.apsusc.2009.01052

Zheng, R. B., Tshabalala, M. A., Li, Q. Y., Wang, H. Y. (2015). "Construction of hydrophobic wood surfaces by room temperature deposition of rutile (TiO_2) nanostructures," *Appl. Surf. Sci.* 328, 453-458. DOI: 10.1016/j.apsusc.2014.12.083

Article submitted: July 2, 2015; Peer review completed: Aug. 26, 2015; Revised version received and accepted: Aug. 27, 2015; Published: September 2, 2015.
DOI: 10.15376/biores.10.4.7053-7064